Characterization of Cross Modulation in Multichannel Amplifiers Using a Statistically Based Behavioral Modeling Technique

Khaled M. Gharaibeh, *Student Member, IEEE,* and Michael B. Steer, *Fellow, IEEE*

***Abstract*—A statistically based modeling technique is developed for characterizing in-band and out-of-band intermodulation and cross-modulation distortions in multichannel amplifier environments. The model is based on a new multiple envelope memoryless behavioral model that captures the black-box characteristics of multichannel amplifiers. A power amplifier with a two code-division multiple-access channel signal is characterized experimentally and verifies the approach.**

***Index Terms*—Behavioral modeling, code division multiple access (CDMA), cross-modulation distortion, multichannel, nonlinear systems, power amplifiers, statistical modeling.**

I. Introduction

THE interaction of multiple signals caused by nonlinear devices leads to cross modulation and is a fundamental performance-limiting phenomena in wide-band multichannel wired and wireless communication systems. The same phenomenon is responsible for co-site interference, intentional and unintentional jamming, and limits what can be achieved with multifunctional systems. In a wireless-power-controlled system such as a code-division multiple-access (CDMA) system, a forward-link multichannel power amplifier is driven by multiple channels that have different power levels because of the near–far problem. In this case, amplitude modulation is transferred from the high-power signal to the low-power signal when the amplifier exhibits a nonlinear nature.

In the traditional multichannel configuration, shown in Fig. 1(a) [1], the individual channels are applied to individual narrow-band power amplifiers and then the outputs of each are combined to obtain a multichannel high-power signal. Generally, zonal filters are used with each narrow-band power amplifier prior to power combining to eliminate out-of-band distortion and, in particular, to eliminate the presentation of undesired signals to the output nonlinearity of the amplifiers. A multichannel amplifier amplifies several channels simultaneously [see Fig. 1(b)], and is expected to be a much lower cost and smaller way of generating the high-power composite signal. However, it is difficult to achieve the low levels of distortion required in advanced wireless systems such as wide-band CDMA systems. One critical problem is that the peak-to-average ratio (PAR) is greater when there are multiple channels than when there is a single channel. Thus, saturation and limiting effects occur at lower average power levels than when there is a single-channel signal. A second problem that arises is the cross modulation and intermodulation that result from interaction of the multiple channels in a nonlinear environment. These manifest themselves as extra in-band and out-of-band distortions.

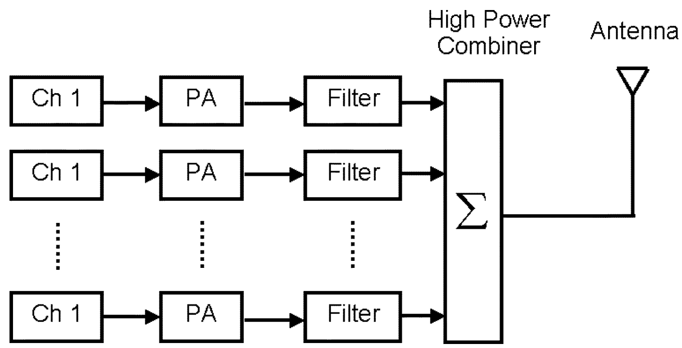

(a)

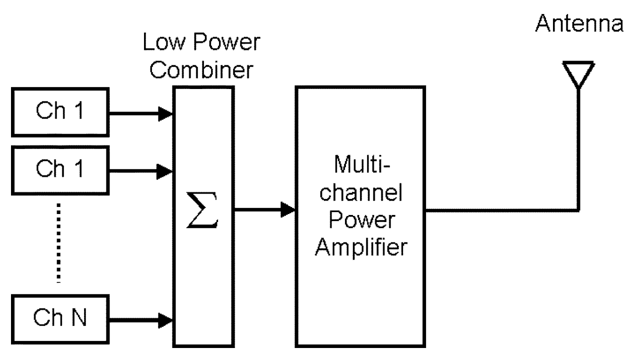

(b)

Fig. 1. Multichannel architectures. Traditional: (a) multiple single-channel amplifier system and (b) single multichannel amplifier system.

In a receiver, the interaction of multiple channels because of nonlinearity manifests itself as a desensitization problem. For example, one of the stringent requirements in CDMA receiver design is the proper reception of a CDMA channel in the presence of a single-tone jammer [2], as shown in Fig. 2. Here, the single-tone desensitization is a measure of the receiver's ability to receive a CDMA signal at its assigned channel frequency and in the presence of a single-tone jammer at a given frequency offset from the CDMA signal center frequency, as shown in

Manuscript received April 14, 2003. This work was supported by the National Science Foundation under Grant CCR-0120319 and by the Army Research Laboratory and Army Research Office as a Multidisciplinary University Research Initiative on Multifunctional Adaptive Radio Radar and Sensors under Grant DAAD19-0101-0496.

The authors are with the Department of Electrical and Computer Engineering, North Carolina State University, Raliegh, NC 27695-7911 USA.

Digital Object Identifier 10.1109/TMTT.2003.819195

0018-9480/03$17.00 © 2003 IEEE

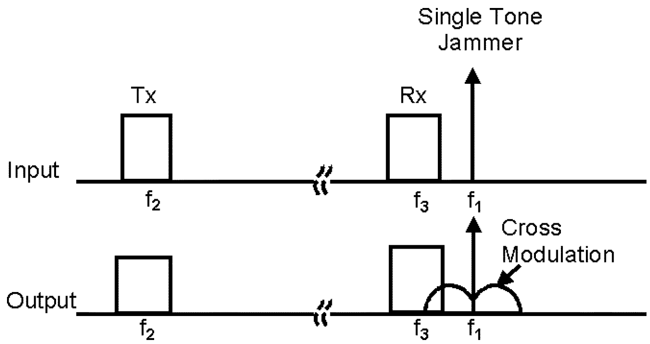

Fig. 2. Receiver desensitization in reverse-link CDMA system.

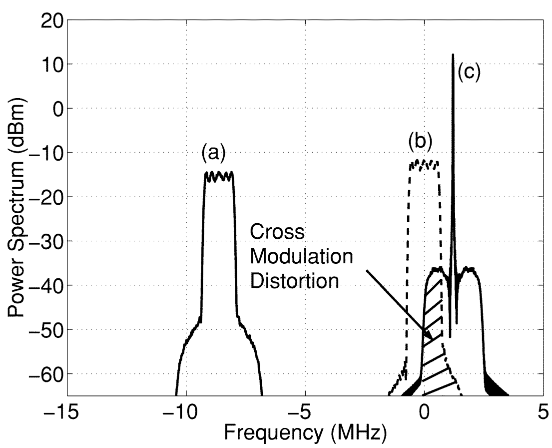

Fig. 3. Simulated cross modulation in reverse-link CDMA system. (a) Tx leakage signal. (b) Received signal. (c) Single-tone jammer.

Fig. 3. The single-tone jammer models a narrow-band advanced mobile phone service (AMPS) signal transmitted from a nearby AMPS base station. The interference introduced by the jammer results from the cross modulation of the jammer and transmitter leakage, which, in turn, appears as extra distortion inside the band of the received signal.

This paper specifically focuses on developing a generalized model for estimating distortion introduced by nonlinearity in a multichannel environment. We discuss two scenarios that are encountered in CDMA systems. The first is a forward-link multichannel amplifier approach, which is preferred for generating high-power signals in base stations. The second situation considered is the receiver desensitization problem in mobile receivers. We extend an analysis for estimating single-channel amplifier distortion [4] to a multiple-envelope statistical technique for estimating distortion in multichannel systems. A general nonlinear spectral analysis is presented for the output signal when the input is the sum of two or more digitally modulated carriers passed through a memoryless nonlinear model. The model is verified by considering a wide-band power amplifier excited by two CDMA channels centered at 2.0 and 2.1 GHz and measuring the adjacent channel power ratio (ACPR) at 2.1 GHz.

In summary, this paper derives the autocorrelation function, by which the output spectrum can be developed, at the output of the nonlinear device using a memoryless nonlinear model. The advance reported here is in the extension of the autocorrelation analysis to a signal comprised of multiple channels and in the development of a parameter-extraction technique for the behavioral model that is suited to multichannel amplifiers.

II. Background

The traditional approach to characterizing distortion in multichannel power amplifiers is to test the amplifier with n tones and examine the intermodulation capability of the power amplifier [5]. However, this cannot accurately characterize cross modulation when the amplifier is driven by digitally modulated signals. Aparin and Larson [2] studied cross-modulation distortion in CDMA receivers due to transmitter (Tx) leakage and the presence of a strong jammer in the receiver band. The analysis of cross-modulation distortion was based on Volterra-series analysis to capture the frequency-dependent characteristics of the amplifier. However, the analysis assumed that the power amplifier is weakly nonlinear and, therefore, Volterra kernels of orders higher than three were neglected because of the increasing complexity. Wang and Brazil [6] simulated the output power spectrum of a nonlinear power amplifier using fifth-order Volterra-series analysis. They simulated the intermodulation output spectrum under two channel CDMA excitation with 5-MHz isolation bandwidth. They also simulated the cross-modulation effect, which is caused by the transfer of the modulation of one signal onto another, but no estimates for that effect on in-band channel distortion were given. In [7], Ko *et al.* derived an empirical formula for estimating the cross-modulation power distortion caused by the presence of single-tone jammer and TX leakage in CDMA mobile phones. The analysis was done assuming third-order nonlinearity. They studied the relation between cross-modulation distortion and the third-order intercept point (IP3) of a low-noise amplifier (LNA) where it was shown that, to overcome cross modulation, an IIP3 of 4–5 dBm of an LNA is required with duplexer isolation of 50 dB. The major problem with all of the above investigations is the relatively low order of the nonlinearity that was considered. Through the general statistical work presented in this paper, this restriction is removed, and it is shown that distortion, including cross modulation, is related to the statistical properties of the signals.

III. CDMA Forward-Link Signal Model and Statistics

The modulation scheme of the IS-95 forward-link CDMA system is shown in Fig. 4. Baseband coded user data is generated at a rate of 19.2 kb/s [8]. Each users' data is first spread by a Walsh code providing orthogonality and then these are logically summed to yield the composite signal at a rate of 1.2288 Mc/s. The resulting data stream is split into in-phase (I) and quadrature (Q) channels, spread by the orthogonal pseudonoise (PN) codes generated at a rate of 1.2288 Mc/s and then passed through a baseband filter. The PN codes are base-station specific and are used with each carrier. The IS-95 baseband pulse-shaping filter can be approximated by an impulse response $h(t) = B\mathrm{sinc}(Bt)$, where $\mathrm{sinc}(x) = (\sin(\pi x)/\pi x)$ and B is the reciprocal of the

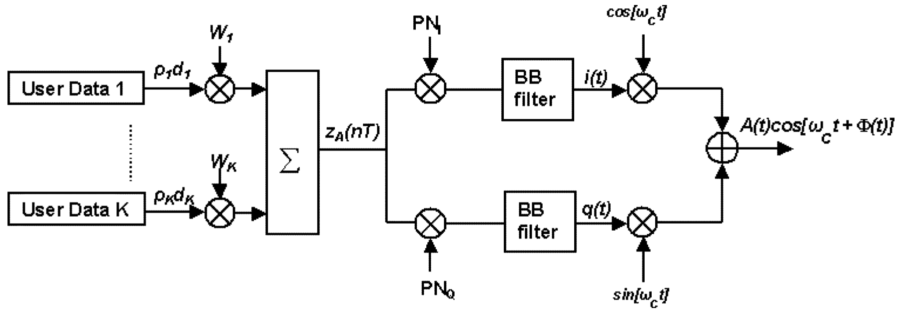

Fig. 4. Block diagram of forward-link IS-95 CDMA system.

PN code rate (1.2288 MHz) [3]. The filtered I and Q channels are quadrature modulated at the carrier frequency and the transmitted signal can be written as

$$\begin{aligned} w(t) &= i(t)\cos(\omega_c t) + q(t)\sin(\omega_c t) \\ &= A(t)\cos\left(w_c t + \Phi(t)\right) \\ &= \frac{1}{2}\left[z(t)e^{j\omega_c t} + z^*(t)e^{-j\omega_c t}\right] \end{aligned} \tag{1}$$

where

$$z(t) = i(t) + jq(t) = A(t)e^{j\Phi(t)}$$

is the complex envelope of the modulated signal $w(t)$. The complex envelope $z(t)$ has a bandwidth B and can be written as

$$z(t) = \frac{1}{\sqrt{2}}\sum_{-\infty}^{\infty} z_A(nT)\left[I(nT) + jQ(nT)\right]h\left(t - nT + \frac{\varphi}{\pi}\right)$$

where $T = T_b/K$ is the chip time, T_b is the bit time, and K is the length of the Walsh code. $I(nT)$ and $Q(nT)$ represent the PN code chips and φ is a random phase uniformly distributed in $[0, 2\pi]$ independent of the sampled process $z_A(nT)$. This signal represents the sampled coded CDMA signal and can be expressed as

$$z_A(nT) = \sum_{i=0}^{K-1} \rho_i d_i(nT)W_i(nT) \tag{2}$$

where d_i are random numbers taking the values ± 1 with equal probability and represent the ith user's data. Each $d_i(nT)$ is constant within the bit period, i.e., $d_i(nT) = \pm 1$ for $0 \leq n \leq K$. $W_i(nT)$ are the Walsh code chips of the ith user. The quadrature components $i(t)$ and $q(t)$ can now be written as

$$\begin{aligned} i(t) &= \frac{1}{\sqrt{2}}\sum_{-\infty}^{\infty} z_A(nT)I(nT)h\left(t - nT + \frac{\varphi}{\pi}\right) \\ q(t) &= \frac{1}{\sqrt{2}}\sum_{-\infty}^{\infty} z_A(nT)Q(nT)h\left(t - nT + \frac{\varphi}{\pi}\right). \end{aligned} \tag{3}$$

The statistics of the CDMA signal are defined by its autocorrelation function. The autocorrelation of the quadrature process $z(t)$ is defined as

$$\begin{aligned} R_{zz}(t, t+\tau) &= E\left[z(t)z^*(t+\tau)\right] \\ &= E\Big[\left\{i(t) + jq(t)\right\}\left\{i(t+\tau) - jq(t+\tau)\right\}\Big] \\ &= R_{ii}(t, t+\tau) - jR_{iq}(t, t+\tau) \\ &\quad + jR_{qi}(t, t+\tau) + R_{qq}(t, t+\tau) \end{aligned}$$

where E is the expected value. Using (3), the autocorrelation functions of the real processes $i(t)$ and $q(t)$ can be written as

$$\begin{aligned} R_{ii}(t, t+\tau) &= \frac{1}{2}E\sum_n\sum_m z_A(nT)z_A(mT) \\ &\quad \times I(nT)I(mT)h\left(t - nT + \frac{\varphi}{\pi}\right) \\ &\quad \times h\left(t - mT + \tau + \frac{\varphi}{\pi}\right) \\ R_{iq}(t, t+\tau) &= \frac{1}{2}E\sum_n\sum_m z_A(nT)z_A(mT) \\ &\quad \times I(nT)Q(mT)h\left(t - nT + \frac{\varphi}{\pi}\right) \\ &\quad \times h\left(t - mT + \tau + \frac{\varphi}{\pi}\right) \\ R_{qq}(t, t+\tau) &= \frac{1}{2}E\sum_n\sum_m z_A(nT)z_A(mT) \\ &\quad \times Q(nt)Q(mT)h\left(t - nT + \frac{\varphi}{\pi}\right) \\ &\quad \times h\left(t - mT + \tau + \frac{\varphi}{\pi}\right) \\ R_{qi}(t, t+\tau) &= \frac{1}{2}E\sum_n\sum_m z_A(nT)z_A(mT) \\ &\quad \times Q(nt)I(mT)h\left(t - nT + \frac{\varphi}{\pi}\right) \\ &\quad \times h\left(t - mT + \tau + \frac{\varphi}{\pi}\right). \end{aligned} \tag{4}$$

The above autocorrelation functions can be evaluated using the statistical properties of data sequences, Walsh codes, and PN codes. The statistical properties of the PN sequences for the forward link are similar to those of the reverse link, which are given by [3]

$$E\big[I(n)I(m)\big] = E\big[Q(n)Q(m)\big] = \begin{cases} 1, & \text{if } n = m \\ 0, & \text{otherwise} \end{cases}$$

and $E[I(n)Q(m)] = E[Q(n)I(m)] = 0$ for all n and m. Therefore, the autocorrelation functions in (4) reduce to

$$\begin{aligned} R_{ii}(t,t+\tau) &= \frac{1}{2}\sum_n E\big[z_A(nT)^2\big] \\ &\quad \times E_\varphi\left[h\left(t-nT+\frac{\varphi}{\pi}\right)h\left(t-nT+\tau+\frac{\varphi}{\pi}\right)\right] \\ R_{qq}(t,t+\tau) &= \frac{1}{2}\sum_n E\big[z_A(nT)^2\big] \\ &\quad \times E_\varphi\left[h\left(t-nT+\frac{\varphi}{\pi}\right)h\left(t-nT+\tau+\frac{\varphi}{\pi}\right)\right] \\ R_{iq}(t,t+\tau) &= 0 \\ R_{qi}(t,t+\tau) &= 0. \end{aligned} \tag{5}$$

Now, the statistics of the sampled process $z_A(nT)$ are known since $z_A(nT)$ represents the input coded data. To find the expected values in (5), we use the statistics of the data samples and Walsh codes. Using (2)

$$\begin{aligned} E\big[z_A^2(nT)\big] &= \sum_{i,j}^{K-1} E\big[\rho_i\rho_j d_i(nT)d_j(nT)W_i(nT)W_j(nT)\big] \\ &= \sum_{i,j}^{K-1} \rho_i\rho_j E\big[d_i(nT)d_j(nT)\big] \\ &\quad \times E\big[W_i(nT)W_j(nT)\big]. \end{aligned} \tag{6}$$

The data sequences d_i are assumed to be independent identically distributed random variables (iid) and independent from the Walsh codes [9], therefore,

$$E\left[d_i(nT)d_j(nT)\right] = \begin{cases} 1, & \text{if } i = j \\ 0, & \text{otherwise.} \end{cases} \tag{7}$$

The statistical properties of Walsh codes are discussed in [9]. Each Walsh code is generated from a set of Hadamard basis functions resulting in orthogonal codes. It follows that (5) reduces to

$$E\left[z_A^2(nT)\right] = \sum_{i=0}^{K-1} \rho_i^2 = \sigma_z^2. \tag{8}$$

The phase φ is assumed to be random and uniformly distributed in $[0, 2\pi]$. Using the properties of the joint moments of pulse trains [3], we have

$$E_\varphi\left[\sum_n\left[h\left(t-nT+\frac{\varphi}{\pi}\right)h\left(t-nT+\tau+\frac{\varphi}{\pi}\right)\right]\right] = h(\tau).$$

Consequently, (8) reduces to

$$\begin{aligned} R_{ii}(\tau) &= \frac{1}{2}\sigma_z^2 h(\tau) \\ R_{qq}(\tau) &= \frac{1}{2}\sigma_z^2 h(\tau) \\ R_{iq}(\tau) &= R_{qi}(\tau) = 0 \end{aligned}$$

and it follows that the autocorrelation function is

$$R_{zz}(\tau) = \sigma_z^2 h(\tau). \tag{9}$$

Therefore, $z(t)$ is a wide sense stationary (WSS) random process since the autocorrelation function $R_{zz}(\tau)$ is a function of the time shift (τ) only. In fact, it is the random phase φ that makes the process a WSS process. If this phase variation does not exist, then the process is considered as a cyclostationary process with the bit period T_b. However, this affects only the higher order moments and not the second-order statistics $(R_{zz}(\tau))$, which is still stationary (independent of time) and, therefore, the analysis above is still valid.

To establish the cross-correlation function of two CDMA signals, let the complex envelopes of the two signals be

$$\begin{aligned} z(t) &= i(t) + jq(t) = A(t)e^{j\Phi_z(t)} \\ u(t) &= r(t) + js(t) = B(t)e^{j\Phi_u(t)}. \end{aligned} \tag{10}$$

The cross-correlation function $R_{uz}(\tau)$ is defined as

$$\begin{aligned} R_{uz}(\tau) &= E\big[z(t)u^*(t+\tau)\big] \\ &= \sum_n\sum_m E\big[z(nT)u^*(mT)\big] \\ &\quad \times h\left(t-nT+\frac{\varphi}{\pi}\right)h\left(t-mT+\tau+\frac{\varphi}{\pi}\right) \end{aligned} \tag{11}$$

where, by using (5),

$$\begin{aligned} E\big[z(nT)u^*(mT)\big] &= E\Big[z_A(nT)\big\{I(nT)+jQ(nT)\big\} \\ &\quad \times u_A(mT)\big\{I(mT)-jQ(mT)\big\}\Big] \\ &= E\big[z_A(nT)u_A(nT)\big]. \end{aligned} \tag{12}$$

The cross-correlation function of the sampled processes $z_A(nT)$ and $u_A(nT)$ can be evaluated now using the definition of the sampled processes $z(nT)$ and $u(nT)$ in (5) and knowing the cross-correlation properties of the data sequences and Walsh codes of the two channels, therefore,

$$\begin{aligned} E\big[z_A(nT)u_A(nT)\big] &= \sum_{i,j}^{K-1} E\big[\rho_i\xi_j d_i^z(nT)d_j^u(nT) \\ &\quad \times W_i(nT)W_j(nT)\big] \\ &= \sum_{i,j}^{K-1} \rho_i\xi_j E\big[d_i^z(nT)d_j^u(nT)\big] \\ &\quad \times E\big[W_i(nT)W_j(nT)\big] \end{aligned}$$

where d_i^z and d_i^u represent the data bits of the ith user in the first and second channels, respectively. Now, assuming that the data bits of the two channels are statistically independent yields

$$E\left[d_i^z(nT)d_j^u(nT)\right] = E\left[d_i^z(nT)\right]E\left[d_i^u(nT)\right] = 0$$

and it follows that, as expected

$$R_{uz}(\tau) = 0. \tag{13}$$

This result means that two processes u and z are orthogonal when the data samples are independent due to the statistical properties of Walsh codes and PN spreading codes. However, the two processes cannot be considered as uncorrelated or statistically independent unless they are assumed to be Gaussian. This assumption will be discussed in the following sections.

IV. Multichannel Nonlinear Behavioral Model

A memoryless model accurately characterizes a nonlinear system (or device) when it has no significant memory within the signal bandwidth. Such a model can always be represented as a complex power series

$$y(t) = \sum_{n=1}^{N} a_n w^n(t) \tag{14}$$

where a_n is the nth instantaneous complex power series coefficient, $y(t)$ is the output waveform, $w(t)$ is the input signal, and N is the order of nonlinearity. A memoryless instantaneous polynomial coefficients are usually not available, however, their envelope counterparts can be extracted by fitting a polynomial to the single-tone AM–AM and AM–PM characteristics, as described in [4]. The instantaneous behavioral model is related to the envelope behavioral model by a Chebyshev integral [11]. Therefore, since only odd-order envelope coefficients can be obtained from first zone measurements (AM–AM and AM–PM), it follows that only odd-order instantaneous coefficients can be retrieved from their envelope counterparts. Fortunately, the odd-order envelope coefficients are the ones needed in the autocorrelation analysis, which will be discussed in the following section, where all the simulations will be done at the complex envelope level.

In the case of two channel analysis, single-tone characteristics are not sufficient since the envelope coefficients extracted at a certain frequency do not necessarily represent the instantaneous coefficients. In order to establish an envelope model that describes the nonlinear behavior with two channel excitation, consider an input consisting of $w_1(t)$ and $w_2(t)$ applied to an amplifier so that $w(t) = w_1(t) + w_2(t)$. The signals $w_1(t)$ and $w_2(t)$ are modulated RF carriers with center frequencies ω_1 and ω_2, respectively. Let $z(t)$ and $u(t)$ be the complex envelopes of $w_1(t)$ and $w_2(t)$, respectively, then the sum signal can be written in complex envelope form as

$$\begin{aligned} w(t) &= w_1(t)+w_2(t) \\ &= \frac{1}{2}\left[z(t)e^{j\omega_1 t}+z^*(t)e^{-j\omega_1 t}+u(t)e^{j\omega_2 t}+u^*(t)e^{-j\omega_2 t}\right]. \end{aligned} \tag{15}$$

Defining the nonlinear model using the input–output relationship (14), applying the signal in (15), and using multinomial expansion yields

$$w^n(t) = \frac{1}{2^n} \sum_{n_1+n_2+n_3+n_4=n} \binom{n}{n_1, n_2, n_3, n_4} \times \left[z^{n_1} {z^*}^{n_2} u^{n_3} {u^*}^{n_4} e^{j(n_1-n_2)\omega_1 t} e^{j(n_3-n_4)\omega_2 t}\right].$$

Considering the components of the output signal centered at the first carrier, this implies that $(n_1-n_2) = \pm 1$ and $(n_3-n_4) = 0$, therefore, the output complex envelope can be expressed as

$$\tilde{y}^{(1)}(t) = \sum_{n=1}^{N} \sum_{k=0}^{\frac{n-1}{2}} b_{n,k} z^{\frac{(n+1)}{2}-k} {z^*}^{\frac{(n-1)}{2}-k} u^k {u^*}^k \tag{16}$$

where the superscript indicates the carrier number

$$b_{n,k} = \frac{a_n}{2^{n-1}} M(n,k)$$
$$M(n,k) = \binom{n}{\frac{n+1}{2}-k, k, k}$$

and

$$\binom{n}{n_1, n_2, \ldots, n_p} = \binom{n}{n_1}\binom{n-n_1}{n_2}\cdots \cdots\binom{n-n_1-\ldots-n_{p-1}}{n_p}$$

is the multinomial coefficient. The above expression is derived assuming that $\omega_2 - \omega_1 > 2B$ and $\omega_2 < 2\omega_1$ so that the intermodulation products do not lie inside the bandwidth of each of the input signals. The envelope behavioral model in (16) be written as

$$\tilde{y}^{(1)}(t) = zG\left(|z|, |u|\right) \tag{17}$$

where G represents the complex gain compression function, is a function of the levels of both signal envelopes, and can be written as

$$G\left(|z|, |u|\right) = \sum_{n=1}^{N} \sum_{k=0}^{\frac{n-1}{2}} b_{n,k} |z|^{n-2k-1} |u|^{2k}. \tag{18}$$

The new set of coefficients $b_{n,k}$ represents the relationship between the input and output complex envelopes of the first carrier. This formulation is needed because this is, in fact, the model that can be extracted by measurements. In order to extract the model coefficients, we introduce a new technique. The idea is that the input power of the first tone is swept, while the power of the second tone is fixed at a certain power level. The process is repeated for each power step of the second tone. In this way, multiple curves for the nonlinear characteristics (AM–AM and AM–PM conversions) are obtained. A two-dimensional (2-D) curve fitting yields the set of coefficients $b_{n,k}$, as will be shown in Section VI, thus, the multichannel behavioral model is obtained. The number of coefficients is equal to $[(N+1)/2 \times (N+3)/4]$.

V. Statistical Analysis of Distortion

With a digitally modulated signal, distortion introduced by nonlinearities is typically characterized by the level of spectral regrowth (SR). In [10], Gard *et al.* developed a generalized autocorrelation formulation for a single CDMA signal. Here, we extend the analysis to the case of multiple channels. The output autocorrelation function at the first carrier is defined as

$$R_{yy}^{(1)}(\tau) = E\left[\tilde{y}^{(1)}(t)\tilde{y}^{(1)}(t+\tau)\right].$$

Now, let $z_1 = z(t)$, $z_2 = z(t+\tau)$, $u_1 = u(t)$, and $u_2 = u(t+\tau)$, then the autocorrelation function of the signal at the first carrier frequency is

$$R_{yy}^{(1)}(\tau) = E\left[\tilde{y}^{(1)}(z_1,u_1)\tilde{y}^{*^{(1)}}(z_2,u_2)\right].$$

Using (16), the output autocorrelation can be formulated as

$$R_{yy}^{(1)}(\tau) = \sum_{n=1}^{N}\sum_{m=1}^{N}\sum_{l=0}^{\frac{n-1}{2}}\sum_{k=0}^{\frac{m-1}{2}} b_{n,l}b_{m,k}^{*}R_{z_n z_m u_l u_k}(\tau) \quad (19)$$

where

$$R_{z_n z_m u_l u_k}(\tau) = E\left[z_1^{\frac{(n+1)}{2}-l} z_1^{*^{\frac{(n-1)}{2}-l}} z_2^{\frac{(n-1)}{2}-k} z_2^{*^{\frac{(n+1)}{2}-k}} \times u_1^l u_1^{*^l} u_2^k u_2^{*^k}\right]. \quad (20)$$

The above expression reduces to the single-channel formulation (as in [10]) when $u(t) = 0$ and setting k, l to 0.

The autocorrelation analysis is needed to develop the output power spectrum by which distortion is characterized. The nonlinear distortion is manifested as SR and gain compression. The power spectrum of the output signal can be found from the Fourier transform of the autocorrelation function as

$$S_{yy}^{(1)}(f) = \sum_{n=1}^{N}\sum_{m=1}^{N}\sum_{l=0}^{\frac{n-1}{2}}\sum_{k=0}^{\frac{m-1}{2}} b_{n,l}b_{m,k}^{*}S_{nmlk}(f) \quad (21)$$

where

$$S_{nmlk}(f) = \int_{-\infty}^{\infty} R_{z_n z_m u_l u_k}(\tau)e^{-j\omega\tau d\tau}.$$

Expression (21) is a general output power spectral density and consists of $[((N+1)/2)^2 \times ((N+3)/4)^2]$ terms. These terms can be divided into three major groups: the first group represents the linear output with gain compression ($l = 0$, $k = 0$, $n = 1$, or $m = 1$). The second group can be categorized as intermodulation distortion ($l = 0$, $k = 0$, $n > 1$, and $m > 1$). The third group represents the cross-modulation distortion caused by the presence of the second signal ($l > 0$ and $k > 0$). In this way, the development of the statistical model provides accurate characterization of cross-modulation distortion, as will be seen in Section VI. Note that the formulation of the autocorrelation function in (20) provides an insight into the effect of the self and joint statistics of the two signals on the level of distortion. This means that this distortion can be controlled by changing the statistics of the two signals. In a forward-link CDMA system, this can be done by the proper choice of the number of users in the two channels, using a different set of orthogonal codes, or introducing a data coding scheme that will result in better distortion performance, however, this is not the subject of this paper.

The receiver desensitization problem can be treated as a special case of the above analysis. Let the input signal $w(t)$ consist of a single-tone jammer $w_1(t) = A_1 cos(\omega_1 t)$ and a transmitter leakage CDMA signal $w_2(t) = A_2(t)cos(\omega_2 t + \Phi(t))$. Therefore, $z(t) = A_1$ and $u(t) = A_2(t)e^{j\Phi(t)}$ and then the output autocorrelation at the jammer center frequency can be expressed as

$$R_{yy}^{(1)}(\tau) = \sum_{n=1}^{N}\sum_{m=1}^{N}\sum_{l=0}^{\frac{n-1}{2}}\sum_{k=0}^{\frac{m-1}{2}} b_{n,l}b_{m,k}^{*}R_{z_n z_m u_l u_k}(\tau)$$

where

$$R_{z_n z_m u_l u_k}(\tau) = A_1^{n+m-2l-2k}E\left[u_1^l u_1^{*^l} u_2^k u_2^{*^k}\right]. \quad (22)$$

The formulation of the autocorrelation function in (19) is greatly simplified if the input signals are assumed to be Gaussian processes. For this, we use the properties of complex Gaussian random variables to obtain a simplified formulation for the autocorrelation function. Using the orthogonality of the two signals, as proven in (13) and (20), can be written as

$$R_{z_n z_m u_l u_k}(\tau) = E\left[z_1^{\frac{(n+1)}{2}-l} z_1^{*^{\frac{(n-1)}{2}-l}} z_2^{\frac{(n-1)}{2}-k} z_2^{*^{\frac{(n+1)}{2}-k}}\right] \times E\left[u_1^l u_1^{*^l} u_2^k u_2^{*^k}\right].$$

For illustration purposes, we will restrict ourselves to writing down the third-order response, however, this can be generalized to any arbitrary order N. Thus, using (19), the output autocorrelation function for third-order nonlinearity is

$$\begin{aligned} R_{yy}^{(1)}(\tau) = &|b_{1,0}|^2 E\left[z_1 z_2^*\right] + b_{1,0}b_{3,0}^* E\left[z_1 z_2^{*^2} z_2\right] \\ &+ b_{1,0}^* b_{3,0} E\left[z_1^2 z_1^* z_2^*\right] + |b_{3,0}|^2 E\left[z_1^2 z_1^* z_2^{*^2} z_2\right] \\ &+ b_{1,0}b_{3,1}^* E\left[z_1 z_2^*\right] E\left[u_2 u_2^*\right] \\ &+ b_{3,0}b_{3,1}^* E\left[z_1^2 z_1^* z_2^*\right] E\left[u_2 u_2^*\right] \\ &+ b_{1,0}^* b_{3,1} E\left[z_1 z_2^*\right] E\left[u_1 u_1^*\right] \\ &+ b_{3,0}^* b_{3,1} E\left[z_1 z_2 z_2^{*^2}\right] E\left[u_1 u_1^*\right] \\ &+ |b_{3,1}|^2 E\left[z_1 z_2^*\right] E\left[u_1 u_1^* u_2 u_2^*\right]. \end{aligned} \quad (23)$$

If the two processes are Gaussian, then the following property of Gaussian random variables applies [4]:

$$E\left[x_1 x_2 \ldots x_s x_1^* x_2^* \ldots x_t^*\right] = \begin{cases} \sum_\pi E\left[x_{\pi(1)}x_1^*\right] E\left[x_{\pi(2)}x_2^*\right] \ldots E\left[x_{\pi(s)}x_s^*\right], \\ s = t \\ 0, \qquad \text{otherwise.} \end{cases} \quad (24)$$

The summation is over all the permutations π of the set of integers $\{1, 2, \ldots, s\}$. Now, the output autocorrelation function for

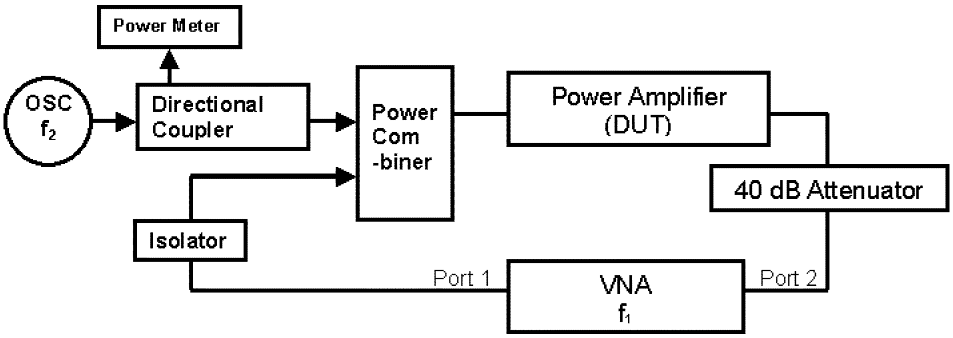

Fig. 5. AM–AM and AM–PM measurement setup.

third-order nonlinearity $(N = 3)$ can be written as (see the Appendix)

$$R_{yy}^{(1)}(\tau) = R_{zz}(\tau)\Big[|b_{1,0}|^2 + 4Re\Big[\big(b_{1,0}b_{3,0}^*\big)\Big]R_{zz}(0) + 2Re\Big[\big(b_{1,0}b_{3,1}^*\big)\Big]R_{uu}(0) + 4Re\Big[\big(b_{3,0}b_{3,1}^*\big)\Big]R_{uu}(0)R_{zz}(0) + 4|b_{3,0}|^2R_{zz}(0)^2 + |b_{3,1}|^2\big(R_{uu}(0)^2\Big] + |b_{3,1}|^2R_{uu}^2(\tau)R_{zz}(\tau) + 2|b_{3,0}|^2R_{zz}^3(\tau). \quad (25)$$

In fact, the autocorrelation function of both a CDMA signal and a narrow-band Gaussian noise (NBGN) process are the same provided that the baseband filter is approximated by a sinc function. The difference is in the evaluation of the higher order moments where the Gaussian assumption enables (24) to be used. The Gaussian approximation is reasonably acceptable for the forward link since the transmitted signal consists of a large number of Walsh-coded data sequences, which, by the central limit theorem, approaches the Gaussian distribution. However, the accuracy of such an approximation decreases if the composite signal is lightly loaded. The accuracy of the Gaussian assumption will be shown in the following section by simulations.

TABLE I
ENVELOPE BEHAVIORAL MODEL COMPLEX COEFFICIENTS

$b_{1,0}$	3.3591-10.7812i
$b_{3,0}$	1.2502+1.2062e2i
$b_{3,1}$	1.4783e1+2.3199e2i
$b_{5,0}$	7.3476e2-5.8665e2i
$b_{5,1}$	-8.5658e2-5.4381e3i
$b_{5,2}$	1.2094e3-1.1498e2i
$b_{7,0}$	-1.6180e4-1.1673e2i
$b_{7,1}$	-9.1893e3+4.6244e4i
$b_{7,2}$	1.3738e4+2.3445e4i
$b_{7,3}$	-9.5786e4-1.5967e5i
$b_{9,0}$	1.2243e5-7.9927e3i
$b_{9,1}$	2.5750e5-1.2319e5i
$b_{9,2}$	-1.1795e5-5.1066e4i
$b_{9,3}$	3.3451e5+8.9860e5i
$b_{9,4}$	2.0552e6+4.4007e6i
$b_{11,0}$	-3.1336e5 +1.1463e5i
$b_{11,1}$	-1.2586e+6-4.9653e4i
$b_{11,2}$	1.1309e5-5.5127e5i
$b_{11,3}$	-6.9983e5-3.8475e6i
$b_{11,4}$	-4.2886e6-8.5872e6i
$b_{11,5}$	-1.5328e7-4.1466e7i

VI. MEASUREMENTS AND SIMULATION RESULTS

The statistical model was used along with the behavioral model coefficients to model the distortion introduced by the interaction of multiple signals in a forward-link IS-95 CDMA system. This section describes the modeling procedure of the above-mentioned concepts.

A. Behavioral Model

The coefficients $b_{n,k}$ in (16) were obtained using a vector network analyzer (VNA) to extract the AM–AM and AM–PM characteristics at $f_1 = 2.1$ GHz of a wide-band C-band amplifier. In addition, an external 2.0-GHz signal source injects a second tone at frequency f_2 at various power levels, as shown in Fig. 5. The AM–AM and AM–PM characteristics at f_1 are determined at each power level of the second source. The power of the VNA signal was swept from -30 to -5 dBm, while the power of the second tone was swept manually from -20 to -5 dBm in 0.5-dB steps and, hence, 30 sets of measurements were obtained. Table I lists the 2-D polynomial coefficients of order $N = 11$, Fig. 6(a) and (b) presents a three-dimensional (3-D) plot of the AM–AM and the AM–PM characteristics as a function of the power levels of both signals and Fig. 6(c) and (d) shows the corresponding polynomial fits. It is worth noting here that this set of coefficients represents the envelope relationship, as in (18), where it is assumed that the output envelope is related to the input envelopes by that equation. A one-to-one relationship between those coefficients and their instantaneous counterparts cannot be developed in this case. If the instantaneous coefficients are sought, the formulation of the problem can be done as a bivariate case, as in [12]. For the sake of this paper, the envelope model in (18) was sufficient, and comparisons between this model and the bivariate case using simulations showed that they give the same result when the analysis is done at the complex envelope level.

B. CDMA Signal Generation

The CDMA signals were generated according to the IS-95 forward-link standard [8]. Sixty-four I and Q random streams

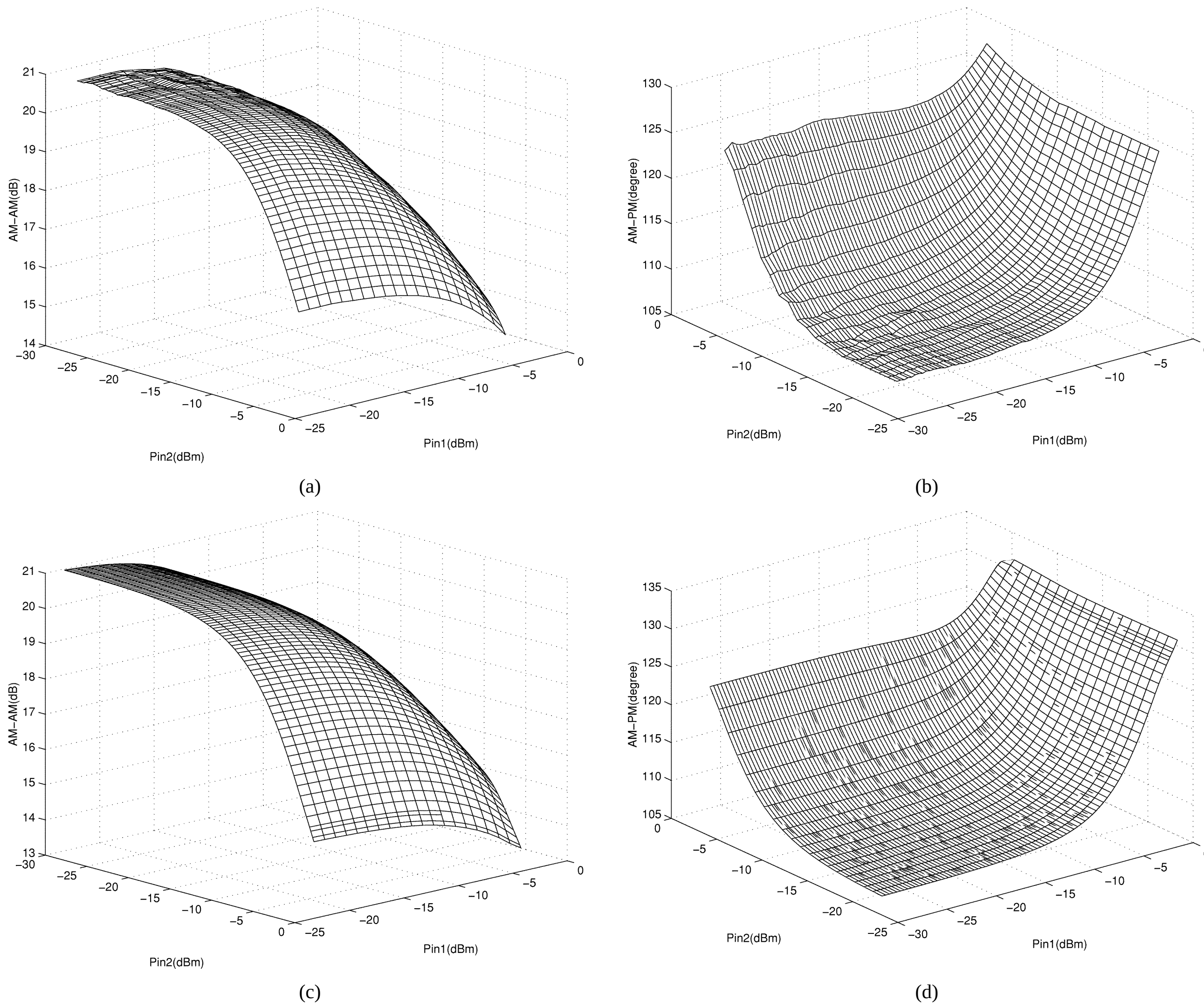

Fig. 6. AM–AM and AM–PM characteristics as a function of the powers of the two tones. (a) and (b) Measured. (c) and (d) Polynomial fit.

each 2^{10}-bit long that represent the data of 64 users were generated in MATLAB. Each bit streams was then multiplied by one of the 64 Walsh codes generated by a 64×64 Hadamard matrix. The spread data streams were logically added and then modulo-2 added to orthogonal PN codes for the I and Q channels. The resulting coded data is then filtered by an IS-95 standard wave-shaping filter.

C. Autocorrelation and Spectrum Estimation

The autocorrelation function of stationary random processes can be obtained from their time averages assuming ergodicity [10]. Therefore, (20) can be evaluated as

$$R_{z_n z_m u_l u_k}(\tau) = \lim_{T\to\infty} \frac{1}{2T} \int_{-T}^{T} z_1^{\frac{(n+1)}{2}-l} z_1^{*\frac{(n-1)}{2}-l} \times z_2^{\frac{(n-1)}{2}-k} z_2^{*\frac{(n+1)}{2}-k} u_1^l u_1^{*^l} u_2^k u_2^{*^k} \, dt. \quad (26)$$

Using the polynomial coefficients developed for the power amplifier in (A), the spectrum of an IS-95 signal was developed using (21). The autocorrelation function and its Fourier transform were computed in MATLAB. Fig. 7 shows the output spectrum of a CDMA signal divided into linear, intermodulation, and cross-modulation components for a CDMA signal centered at 2.1 GHz assuming that the nonlinear model is excited by the sum of two CDMA channels centered at 2.0 and 2.1 GHz. The output spectrum shows the increase in SR and in-channel dis-

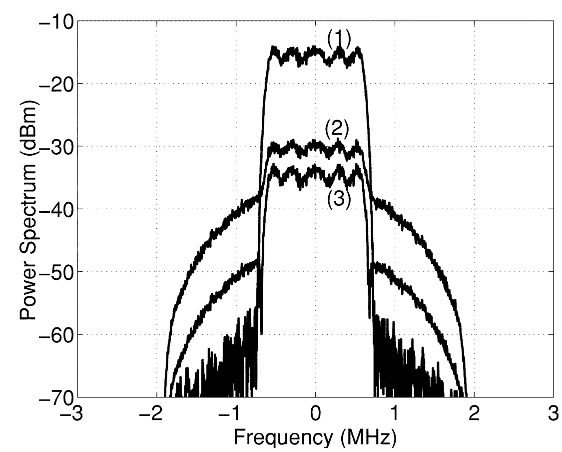

Fig. 7. Output spectrum divided into: (1) linear, (2) cross-modulation, and (3) intermodulation components.

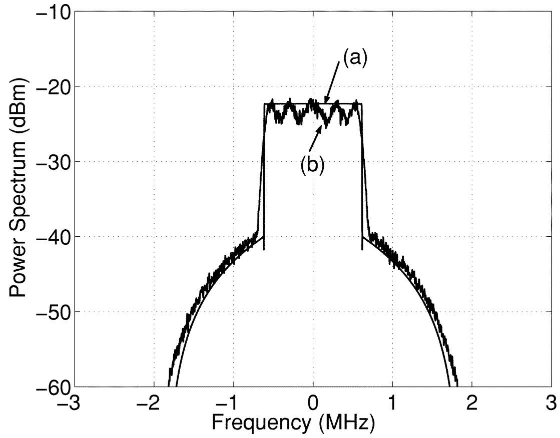

Fig. 8. Output power spectrum using: (a) Gaussian assumption and (b) actual signal realization.

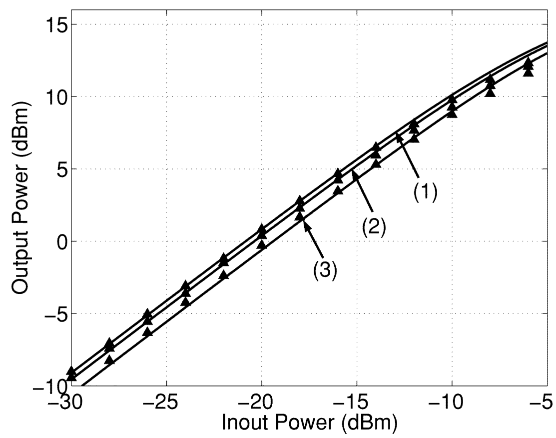

(a)

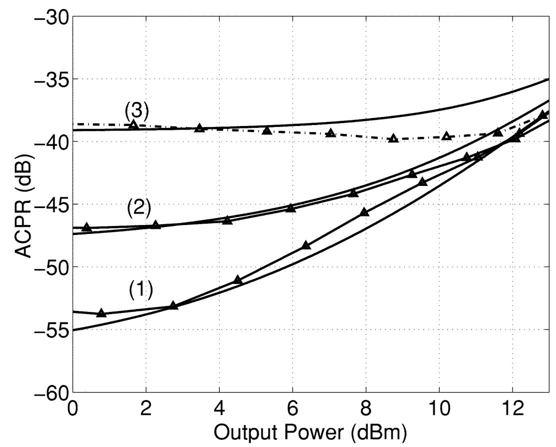

(b)

Fig. 9. (a) Gain compression at the first carrier. (b) ACPR of the first carrier with second carrier at (1) -20, (2) -15, and (3) -10 dBm (Solid: simulated, $\triangle$: measured).

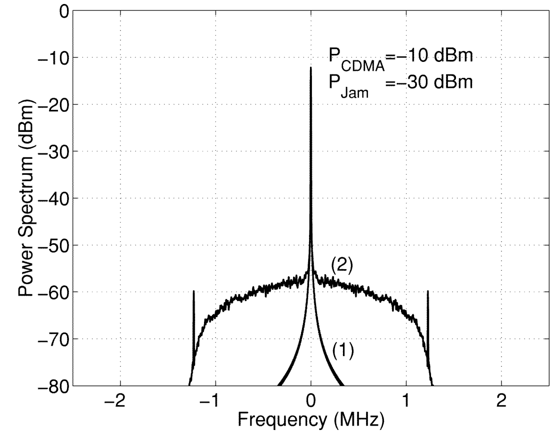

(a)

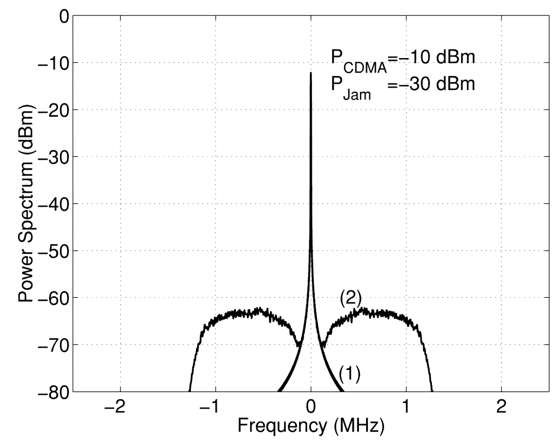

(b)

Fig. 10. Spectrum of a single tone with: (1) no cross modulation and (2) cross modulation by mixing with a CDMA signal. (a) Forward link. (b) Reverse link.

tortion over single-channel excitation due to cross modulation. Fig. 8 shows the output spectrum generated from signal realization and from use of a fully loaded IS-95 forward channel $(K = 64)$ using the time autocorrelation in (26) superimposed on the spectrum generated from the Gaussian assumption, and assuming that $R_{zz}(\tau) = \sigma^2 B \mathrm{sinc}(Bt)$, where it is shown that the Gaussian assumption gives a good estimate of distortion.

The statistical model was verified experimentally as described here. ACPR and gain compression were estimated from the simulated spectrum according to the IS-95 Standard [4]. The amplifier was tested with IS-95 forward channel signals using a vector signal generator (VSG) and a vector signal analyzer (VSA). The amplifier was driven by two IS-95 fully loaded forward-link channels centered at 2.0 and 2.1 GHz. The ACPR measurements were performed for the signal at 2.1 GHz. Fig. 9 shows gain the compression and ACPR of the first channel as a function of its output power and the second channel input power. Close agreement with the statistical nonlinear model is shown at power levels of -20 and -15 dBm of the second signal. At $\mathrm{P}_{\mathrm{in}2} = -10$ dBm, the simulated values differ from measured values by 4 dB in the region where the input power of the first signal is high. This is due to the accuracy of the polynomial model at high power levels where it fails when the input power is beyond the compression region.

D. Receiver Desensitization

Fig. 10 presents the output spectrum of a single tone when the power amplifier is driven by a single tone and a forward-link signal [see Fig. 10(a)] and a single tone with a reverse link signal [see Fig. 10(b)]. The spectrum, developed using (22), shows how the spectrum is widened because of the mixing with

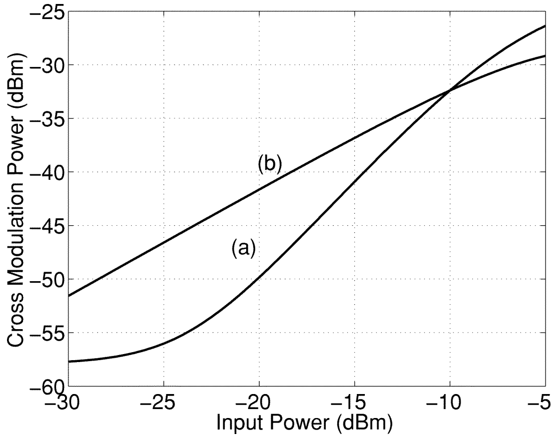

Fig. 11. Cross-modulation power over swept input power. (a) CDMA signal power. (b) Jammer power.

the modulated CDMA carrier as a result the nonlinear interaction or cross modulation. If the CDMA signal is a reverse-link signal, then cross modulation appears as a double hump similar to that predicted in [3] using a circuit-level model. On the other hand, if the CDMA signal is a forward-link signal, then cross modulation appears close to a triangular shape, which is similar to that predicted by the NBGN assumption. This is due to the fact that the NBGN assumption is better suited to modeling the forward link than the reverse link. Fig. 11 shows the cross-modulation power in a 30-kHz bandwidth at an offset of 885 kHz from the center frequency of the single tone. The first curve shows cross-modulation power as a function of swept input power of the CDMA signal (forward link) in a 25-dBm range ($\mathrm{P}_{\mathrm{CDMA}} = -30$ dBm to -5 dBm, $\mathrm{P}_{\mathrm{Jam}} = -10$ dBm), while the second curve shows the cross-modulation power as a function of swept input power of the single-tone jammer itself in the same power range ($\mathrm{P}_{\mathrm{Jam}} = -30$ dBm to -5 dBm, $\mathrm{P}_{\mathrm{CDMA}} = -10$ dBm). The two curves show that the jammer power contributes much more strongly to the cross-modulation power than the power of the CDMA signal.

VII. Conclusion

A generalized statistical analysis for modeling cross modulation in multichannel nonlinear amplifiers has been introduced. In addition, a new behavioral modeling technique for modeling cross modulation in a multichannel nonlinear amplifiers has been presented and verified. The statistical model shows that intermodulation and cross-modulation distortions depend on the statistical properties of the signal, which are captured by the autocorrelation function. In a forward-link CDMA system, distortion depends on the number of data channels (users) and the selection of Walsh codes involved in the composite signal. This is because the transmitted signal exhibits a PAR that depends on the Walsh codes involved in the composite waveform. It has also been shown that the Gaussian assumption results in a simplified analysis of the autocorrelation function, while it gives a good estimate of distortion in the forward link. The analysis that has been presented provides an insight into the design of multichannel amplifiers and CDMA systems.

Appendix

To derive (25), we start by evaluating the following correlation functions:

$$
\begin{aligned}
E\left[z_1 z_2^*\right] &= R_{zz}(\tau)\\
E\left[z_1^* z_2\right] &= R_{zz}(\tau)\\
E\left[z_1 z_1^*\right] &= E\left[z_2 z_2^*\right] = R_{zz}(0)\\
E[z_1 z_2] &= E[z_2 z_2] = 0\\
E\left[u_1 u_2^*\right] &= R_{uu}(\tau)\\
E\left[u_1 u_1^*\right] &= E\left[u_2 u_2^*\right] = R_{uu}(0)\\
E[u_1 u_1] &= E[u_2 u_2] = 0\\
E\left[z_1 u_2^*\right] &= E\left[u_1 z_2^*\right] = R_{uz}(\tau) = 0\\
E[z_1 u_2] &= E[u_1 z_2] = 0.
\end{aligned}
$$

Now, using (24), we evaluate each term in (23) as follows:

$$
\begin{aligned}
E\left[z_1 z_2^*\right] &= R_{zz}(\tau)\\
E\left[z_1 z_2^{*^2} z_2\right] &= 2R_{zz}(0)R_{zz}(\tau)\\
E\left[z_1^2 z_1^* z_2^*\right] &= 2R_{zz}(0)R_{zz}(\tau)\\
E\left[z_1^2 z_1^* z_2^{*^2} z_2\right] &= 2R_{zz}^3(\tau) + 4R_{zz}^2(0)R_{zz}(\tau)\\
E\left[z_1^2 z_1^* z_2^*\right] &= 2R_{zz}(0)R_{zz}(\tau)\\
E\left[z_1 z_2^*\right] &= R_{zz}(\tau)\\
E\left[z_1 z_2 z_2^{*^2}\right] &= 2R_{zz}(0)R_{zz}(\tau)\\
E\left[u_1 u_1^* u_2 u_2^*\right] &= R_{uu}^2(0) + R_{uu}^2(\tau).
\end{aligned}
$$

Collecting the power like terms, (25) follows directly.

References

[1] M. Johansson, T. Mattsson, L. Sundstrom, and M. Faulkner, "Linearization of multi-carrier power amplifiers," in *IEEE 43rd Vehicular Technology Conf.*, 1993, pp. 684–687.

[2] V. Aparin and L. E. Larson, "Analysis and reduction of cross-modulation distortion in CDMA receivers," *IEEE Trans. Microwave Theory Tech.*, vol. 51, pp. 1591–1602, May 2003.

[3] V. Aparin, "Analysis of CDMA signal spectral regrowth and waveform quality," *IEEE Trans. Microwave Theory Tech.*, vol. 49, pp. 2306–2314, Dec. 2001.

[4] K. Gard, H. Gutierrez, and M. B. Steer, "Characterization of spectral regrowth in microwave amplifiers based on the nonlinear transformation of a complex Gaussian process," *IEEE Trans. Microwave Theory Tech.*, vol. 47, pp. 1059–1069, July 1999.

[5] J. S. Kenney and A. Leke, "Design considerations for multicarier CDMA base station power amplifiers," *Microwave J.*, vol. 42, p. 76, 77, 79, 80, 82, 84, 86, Feb. 1999.

[6] T. Wang and T. Brazil, "Using Volterra mapping based behavioral models to evaluate ACI and cross modulation in CDMA communication systems," in *High Frequency Postgraduate Student Colloq.*, Dublin, U.K., Sept. 2000, pp. 102–108.

[7] B. Ko, D. Cheon, S. W. Kim, J. Ko, J. Kim, and B. Park, "A nightmare for CDMA RF receiver: the cross modulation," in *1st IEEE Asia–Pacific Conf. on ASICs*, Seoul, Korea, Aug. 1999, pp. 400–402.

[8] T. S. Rappaport, *Wireless Communications: Principles and Practice*. Englewood Cliffs, NJ: Prentice-Hall, 1996.

[9] R. N. Braithwaite, "Using Walsh code selection to reduce the power variance of band-limited forward-link CDMA waveforms," *IEEE J. Select. Areas Commun.*, vol. 18, pp. 2260–2269, Nov. 2000.

[10] K. Gard, L. E. Larson, and M. B. Steer, "Generalized autocorrelation analysis of spectral regrowth from bandpass nonlinear circuits," in *IEEE MTT-S Int. Microwave Symp. Dig.*, May 2001, pp. 9–12.

[11] M. Jeruchim, P. Balaban, and S. Shanmugan, *Simulation of Communication Systems*. New York: Kluwer, 2000.

[12] P. J. Lunsford, II, "The frequency domain behavioral modeling and simulation of nonlinear analog circuits and systems," Ph.D. dissertation, Dept. Elect. Comput. Eng., North Carolina State Univ., Raleigh, NC, 1993.

[13] P. B. Kenington, *High Linearity Amplifier Design*. Norwood, MA: Artech House, 2000.

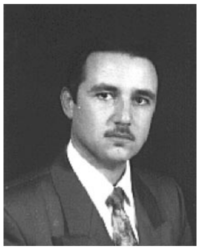

Khaled M. Gharaibeh (S'01) received the B.S. and M.S. degrees in electrical engineering from the Jordan University of Science and Technology, Irbid, Jordan, in 1995 and 1998 respectively, and is currently working toward the Ph.D. degree in electrical and computer engineering at North Carolina State University, Raleigh.

From 1996 to 2000, he was a Senior Engineer with Jordan Telecom, Amman, Jordan. Since May 2000, he has been with the Department Electrical and Computer Engineering, North Carolina State University. His research interests are nonlinear system identification, behavioral modeling of nonlinear RF circuits, and digital communications.

Mr. Gharaibeh is a member of Eta Kappa Nu.

Michael B. Steer (S'76–M'82–SM'90–F'99) received the B.E. and Ph.D. degrees in electrical engineering from the University of Queensland, Brisbane, Australia, in 1976 and 1983, respectively.

He is currently a Professor with the Department of Electrical and Computer Engineering, North Carolina State University, Raleigh. In 1999 and 2000, he was a Professor with the School of Electronic and Electrical Engineering, The University of Leeds, where he held the Chair in microwave and millimeter-wave electronics. He was also Director of the Institute of Microwaves and Photonics, The University of Leeds. He has authored over 240 publications on topics related to RF, microwave and millimeter-wave systems, high-speed digital design, and RF and microwave design methodology and circuit simulation. He coauthored *Foundations of Interconnect and Microstrip Design* (New York: Wiley, 2000).

Prof. Steer is active in the IEEE Microwave Theory and Techniques Society (IEEE MTT-S). In 1997, he was secretary of the IEEE MTT-S. From 1998 to 2000, he was an elected member of its Administrative Committee. He is the Editor-In-Chief of the IEEE TRANSACTIONS ON MICROWAVE THEORY AND TECHNIQUES (2003–2006). He was a 1987 Presidential Young Investigator (USA). In 1994 and 1996, he was the recipient of the Bronze Medallion presented by the Army Research Office for "Outstanding Scientific Accomplishment." He was also the recipient of the 2003 Alcoa Foundation Distinguished Research Award presented by North Carolina State University.